Journal of Structural Geology, Vol. 11, No. 1/2, pp. 163 to 174, 1989
Printed in Great Britain

0191-8141/89 $03.00 + 0.00
Pergamon Press plc

Synkinematic microscopy of transparent polycrystals

W. D. MEANS

Department of Geological Sciences, State University of New York at Albany, 1400 Washington Avenue, Albany, NY 12222, U.S.A.

(*Received* 12 *October* 1987; *accepted* 2 *September* 1988)

Abstract—Deformation of weak, polycrystalline materials in thin section, on the stage of a petrographic microscope, offers insight into the origin of optical microstructures similar to microstructures in naturally deformed rocks. Sample materials used to date include several soft minerals (ice, carnallite, bischofite, nitratite) and various organic plastic materials. They can be simple-sheared or pure-sheared at temperatures to 300°C, at a variety of strain rates, using relatively simple and inexpensive apparatus. The complete microstructural evolution can be recorded photographically, along with the complete kinematic history. Research applications have focussed on dynamic recrystallization, and progress has been made towards understanding how the average grain size is maintained constant in steady-state recrystallization flow. Records have been obtained of the development of various crystal–plastic microstructures and of lattice reorientation trajectories during flow. Teaching applications have begun to be developed, and several videotapes are available. Future technical developments are expected to permit stress measurement or control during experiments, and synkinematic recording of lattice reorientation. Numerous research areas invite attention. These include investigation of the microstructural developments that precede faulting, the behaviour of deforming crystal–melt systems, and the behaviour of dynamically reactive, multi-phase systems.

INTRODUCTION

APPLIED microstructural geology is flourishing. Mappers consult thin sections for otherwise unobtainable sense-of-shear information. Petrologists cite microstructure to tie *P–T–t* curves to deformation history. Geophysical modellers use stress intensities based on grain sizes. Strain analysts work with grain spacings and grain shape orientations. Experimentalists extrapolate rock strengths to orogenic strain rates using microstructurally-justified flow laws.

Basic microstructural geology, on the other hand, is not in so robust a state. There have been advances over the past 20 years (microstructural electron microscopy, computer simulation of fabric development, reading of displacement histories from crystal growth fibers), but there has not been rapid improvement in the level at which we understand small-scale *deformation processes*—by which I mean deformation-induced processes, operating on the grain-scale and below, during and after deformation, that control the microstructures and lattice orientations in deformed rocks. The need is to interest many new participants in research on deformation processes and to develop some fresh approaches to their study. This review describes one such approach, an approach involving microstructural analogs of rocks and synkinematic microscopy.

Microstructural analogs of rocks are materials that develop rock-like microstructure when deformed—for example metals, ceramics and certain organic crystalline materials. Most of what we understand of the principles of microstructural development in rocks has come from mid-20th century experience with analogs, especially metals. Metallurgists, in turn, built their understanding on turn-of-the-century observations of slip in soft crystals by mineralogists (e.g. Mugge 1898). Thus minerals once served as analogs for understanding the behavior of metals. The fruitful transfer of ideas from one group of crystalline materials to another is expected to continue and should be fostered by the kinds of experiments described here.

Experiments with synkinematic microscopy—microscopy during deformation—have advantages and disadvantages relative to conventional experiments. In conventional rock deformation experiments with a microstructural purpose, one deforms a rock sample, thin-sections it, and compares this thin section with a thin section of the same rock in its undeformed condition. Using synkinematic microscopy, one makes a thin section of the *undeformed* material and contrives to deform *this*, while watching it through a microscope. The obvious advantage is that a record can be made of the entire microstructural history, from the undeformed state to the fully deformed state. Independently of the microstructural history, one can record the complete kinematic history—the history of particle motion. Independent measurement of particle motion is important because microstructural change and particle motion are not simply coupled in processes of interest, like dynamic recrystallization or dynamic shrinkage of reactant grains and growth of product grains. The coupling is complex because the structural elements (grain boundaries, subgrain boundaries, phase boundaries) can migrate *through* the material as well as move with it. The challenge to understanding such processes is to work out the physics and chemistry of the coupling between particle motion and the motion of these non-material structural elements. This should be much easier with synkinematic microscopy than with other experimental techniques.

A disadvantage of synkinematic microscopy, from a

geological viewpoint, is that none of the common rock-forming minerals (except ice and perhaps halite) can be studied in their ductile regimes. They are too strong and too brittle under the conditions accessible to synkinematic microscopy (pressures to a few tens of MPa, temperatures to 300°C, at present). Another disadvantage is that it is difficult to measure the bulk mechanical properties of the tiny field of grains that is being viewed microscopically. For these reasons there is an undesirable gap between conventional rock deformation experiments and the experiments described here. There are however two connecting links. There is the possibility, in some materials, of doing conventional experiments on bulk samples along with synkinematic microscopy on thin samples of the same materials and comparing the results, as Urai (1983a) has done with carnallite and Tungatt & Humphreys (1984) have done with nitratite ($NaNO_3$). There is also the microstructural similarity between certain materials observed by synkinematic microscopy and rocks deformed in conventional experiments, suggesting that similar processes may have been active. The reader will see many geological-looking microstructures in the figures of this paper.

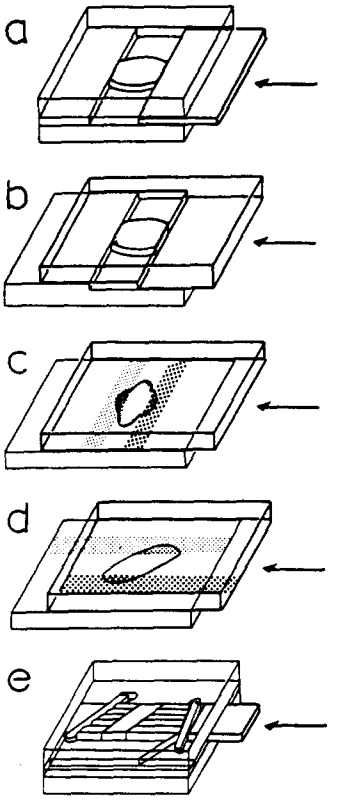

Fig. 1. Various arrangements for containing and loading the sample (grey) in see-through deformation apparatus. (a) Piston pushed between fixed glass windows. (b) Moving windows with steps. (c & d) Moving windows with frosted strips for pure shearing and simple shearing respectively. (e) Burg *et al.* (1986) arrangement for simple shearing (schematic).

TECHNIQUE

Transmitted light microscopy of flowing polycrystals was pioneered 30 years ago by glaciologists deforming ice (Steinemann 1958, Rigsby 1960, Wakahama 1964). It was taken up again by a few geologists and metallurgists about 10 years ago. The techniques in hand are mainly the work of J. Urai (State University of Utrecht), C. Wilson (University of Melbourne) and myself. Published results have come mainly from these three geological centers and from J. Humphreys and co-workers at the Metallurgy Department, Imperial College, London.

The procedure requires a transparent sample and a deformation apparatus through which light can pass from sample to microscope (a 'see-through' deformation apparatus). In current designs the sample is sandwiched between glass windows and deformed there by driving a thin, metal piston between the windows, or by moving the windows relative to one another (Fig. 1).

In the pistonless arrangements (Fig. 1b–d), the windows bear steps or frosted grips which engage the sample and impose a velocity gradient across it. The frosted grip technique is the best so far developed for deforming samples as thin as ordinary thin sections, and thereby obtaining optimal resolution of microstructural detail. The piston techniques (Fig. 1a & e) require thicker samples, since sample thickness equals piston thickness, and pistons thinner than about 70 μm buckle. These techniques are suitable for materials of low birefringence like camphor (Urai *et al.* 1980) or ice (Burg *et al.* 1986, Wilson 1986), for which relatively thick samples are needed for adequate crossed-polars contrast between grains. Using one or another of the arrangements in Fig. 1, large, approximately plane, progressive pure shear or simple shear deformations can be imposed upon samples, with the direction of intermediate strain conveniently parallel to the microscopists's line of sight.

Several kinds of motorized presses for driving the piston or one of the windows have been used (see brief descriptions in Means & Xia 1981, Wilson 1984, Burg *et al.* 1986). The state-of-the-art, general purpose press, not yet described in the literature, is the Urai press shown in Fig. 4(a) and available commercially from E. de Graaf (Rembrandtlaan 13, 3723 BG Bilthoven, The Netherlands). This is a compact, stage-mounted press with interchangeable motors for different strain rates (10^{-4}–10^{-6} s^{-1} or lower) and a heating system for maintaining the sample at temperatures to 300°C. In this and other current apparatus, a small normal stress (of the order of 0.1 MPa) is imposed upon the sample by the windows but otherwise there is no confining pressure. A design for confining pressure to a few tens of MPa was described by Means (1977) but has not been used recently.

Ordinary petrographic microscopes are employed, except by Wilson and co-workers who use an inverted microscope and thereby obtain a larger working space between light source and sample. The Urai press will fit on any ordinary petrographic microscope that accepts a universal stage.

Sample materials generally need to be optically aniso-

Table 1

Name	Composition	Crystal system	Melting (M) or decomposition (D) point (°C)
Ice	H_2O	Hexagonal	0 (M)
Bischofite	$MgCl_26H_2O$	Monoclinic	(D)
Carnallite	$KMgCl_36H_2O$	Orthohombic	(D)
Nitratite	$NaNO_3$	Rhombohedral	306 (M)
Paradichlorobenzene	$C_6H_4Cl_2$	Triclinic > 31	51 (M)
		Monoclinic < 31	
Octachloropropane	C_3Cl_8	Hexagonal	160 (M)
Camphor	$C_{10}H_{16}O$	Cubic > 92	
		Rhombohedral < 92	179 (M)
Biphenyl	$C_6H_5C_6H_5$	Monoclinic	70 (M)

tropic (for crossed-polars imaging of microstructure) and mechanically weak (for yielding before a window or piston does). Weakness is ensured by picking sample materials with low melting points (~300°C or below). Such materials tend to be soft and ductile, even at temperatures not far from room temperature.

Four minerals and four non-minerals have received most attention to date: ice, carnallite, bischofite and nitratite; camphor, paradichlorobenzene, octachloropropane and biphenyl. Table 1 gives their compositions and other properties. The non-minerals are organic materials from a group called *organic plastic crystals*. They appear to undergo ductile deformation by the same kinds of dislocation and diffusion processes as minerals, metals and ceramics (Sherwood 1979 and references therein).

Samples down to about 60 μm in thickness can be cut, ground and transferred to the apparatus for deformation. Samples thinner than this are too fragile for handling and need to be prepared between the windows where they will be deformed. Procedures include crystallization from melt films and hot-pressing, with various thermal or aging treatments to obtain desired initial grain sizes and microstructures. Details are given for individual materials in the references. Sample preparation is one of the most challenging (and educational) parts of the work, since manipulating microstructure depends on knowing the very principles one is out to discover. There is a degree of circularity in the work, and an element of luck when success is achieved.

Marker objects for following particle motion are sometimes spontaneously present in the samples (like the bubbles in the sodium nitrate grains of Tungatt & Humphreys 1984 and the ice of Burg *et al.* 1986). Otherwise they can be inserted by mixing fine particles of a second phase in the melt or powder from which the sample is prepared. Silicon carbide grinding powder is one suitable marker material. It stands out well in plain light photomicrographs, and has particles of more or less uniform size but varied shapes. The shape variation facilitates correlation of markers from one photo to another. The markers do not seem to impede migration of grain or subgrain boundaries in my experience, so long as they are fine enough (1000-grit preferred) and not clotted together. The assumption made in using the second phase particles to follow the pattern of motion in the main phase is that a given marker particle remains surrounded by the same main-phase atoms throughout a deformation history (give or take a few atoms which move in or out diffusively). Where most of the atoms are moving diffusively but in a co-ordinated way (in one general direction at any marker site, as in volume-diffusion creep), it is assumed that here too, the marker will stay surrounded by about the same population of atoms. However, the establishment of material reference frames in diffusion flow situations, especially where different species are diffusing at different rates or in different directions, is not going to be straight-forward.

Figure 4(b–h) illustrates the range of microstructures that can be studied. Figure 4(b) shows part of a polycrystal of octachloropropane (OCP) that has been deformed at room temperature by poking it with a needle. In this plain light view the grain boundaries are visible but deformation effects are not evident except for the needle track itself, in the upper left-hand corner. Figure 4(c) shows the crossed-polars view of the same field and reveals some crystal–plastic microstructures around the needle track. A deformation band extends horizontally across the central dark grain, and local lattice reorientation is also evident in other grains, from unevenness in their interference shades. Features optically similar to deformation lamellae are sometimes seen inside the deformation bands. An example is shown in Fig. 4(d). As in quartz, the lamellae in OCP are usually parallel or about parallel to the trace of the basal plane, and the deformation band boundaries are about parallel to the trend of the *c*-axis. Figure 4(e) shows a set of mica-like kink bands wrinkling the basal plane in a single crystal of biphenyl shortened horizontally, at room temperature. Figure 4(f) shows rhombohedral cleavage cracks (black, subvertical) and mechanical twin lamellae (grey, subhorizontal) in a single crystal of sodium nitrate deformed at room temperature. Sodium nitrate is a particularly appealing starting material because it is isostructural with calcite and displays a range of behaviors from somewhat brittle, as here, to fully ductile at temperatures from about 200°C upwards to its 306°C melting point (Tungatt & Humphreys 1981 a, b, 1984). This whole temperature range is accessible to synkinematic microscopy using current apparatus.

Figure 4(g & h) shows an example of the ease with which recrystallization effects are obtained in some of these materials. Figure 4(g) shows an uncovered OCP sample that was scratched by rubbing it lightly with tissue paper. Figure 4(h) shows the crossed-polars view of the same field, just a few minutes later. Many small, new grains have grown by recrystallization of the strongly deformed OCP along the larger scratches.

RESEARCH APPLICATIONS

The main process studied to date by synkinematic microscopy has been dynamic (synkinematic) recrystallization. Many familiar and expected phenomena have been seen, such as grain-size reduction by dynamic recrystallization (in camphor by Urai *et al.* 1980; in sodium nitrate by Tungatt & Humphreys 1981b; and in ice by Wilson 1986) and recrystallization of single crystals by a process involving progressive misorientation of subgrains (Fig. 4i–l). These phenomena have been observed closely for the first time, as have some details of dynamic nucleation by bulge processes (Means 1981, fig. 3, Tungatt & Humphreys 1984, fig 13).

The main novel contribution of synkinematic microscopy to understanding dynamic recrystallization has been the observation for the first time of processes that are expected to maintain a constant grain size and lattice preferred orientation in steady-state dynamic recrystallization. I refer to experiments like those of Urai (1987, on wet bischofite) in which deformation was carried on long enough after initial reduction of grain size to see how the new grains then interacted with each other, and to experiments like Jessell's (1986a, on octachloropropane) in which the initial grain size was close enough to the steady-state grain size so that no 'duplex structure' forms (no new grains of distinctly smaller size than the old grains). What happens in these circumstances is that *large-wavelength bulges* develop along grain boundaries. These are bulges with a half-wavelength (bulge width) of the same order as the grain radius. These bulges migrate through the material, continuously converting parts of it from one lattice orientation to another (see Means 1983, fig. 4, Urai 1983a, fig. 14). This is a kind of recrystallization that produces no new grains (in the sense of initiating a grain at a very small bulge or subgrain) but it is a recrystallization process by current definitions (Haessner & Hoffman 1978, Urai *et al.* 1986). It is expected to be a mechanical softening process like other kinds of recrystallization. The grains are non-material 'orientation domains' (Urai *et al.* 1986) that move around through the material and each other in a complex manner. Figure 2 shows examples of large wavelength bulge migration in OCP. The grains are named numerically in the starting material (Fig. 2a), and one can see that even at about 50% shortening (Fig. 2d) all the grains present are original grains. (The correlations shown by the numbers are based on about 40 color photomicrographs between a and d, which allows the changing shapes and positions of the grains to be followed with confidence.) Many of the original grains have been consumed by their neighbors, but no new grains have been introduced.

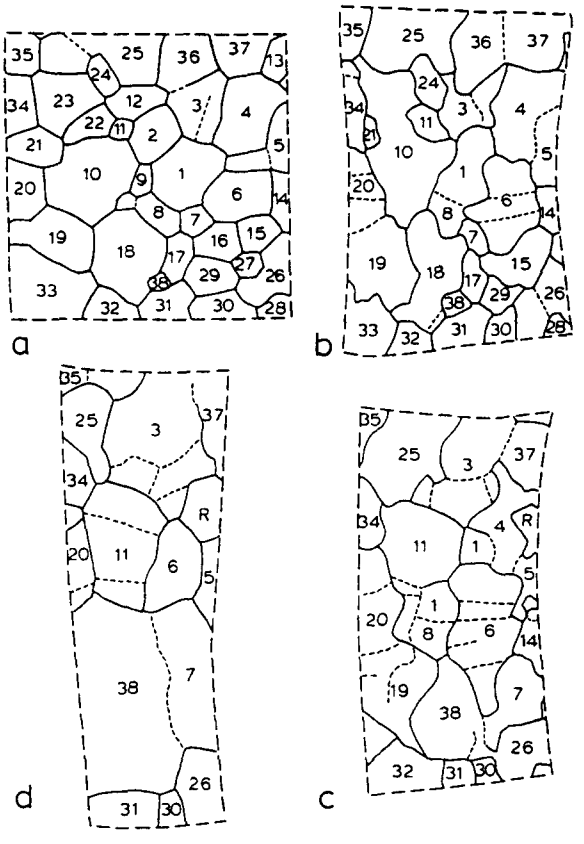

Fig. 2. Changing grain shapes and sizes in an original square millimeter (a) of a dynamically recrystallizing OCP sample, pure-sheared at room temperature, 2×10^{-5} s^{-1} strain-rate. The bulk strain at each subsequent stage (b), (c) & (d) can be seen from the changed shape of mapped area. Area changes are associated with small extensions normal to page. Numbers identify grains from map to map. Subgrain boundaries marked with short dashes. Grain R in (c & d) migrated into mapped area from right. Microstructural developments in this sample to 30% bulk shortening were described by Means (1983).

The grain size in Fig. 2 is not steady but three phenomena are seen which are expected to play a role in the maintenance of a constant average grain size in steady-state dynamic recrystallization: dissection, coalescence and amalgamation. *Dissection* (Urai *et al.* 1986, Urai 1987, fig. 7) is exhibited in Fig. 2(b & c) where grain 1 becomes divided into separate parts by growth across it of other grains. *Coalescence* is shown in Fig. 2(b–d) where similarly-oriented grains 7 and 38 grow to impingement by consuming intermediate grains. Because they are similarly oriented, the impingement boundary becomes a subgrain boundary in the 7–38 supergrain. Another example of coalescence is provided by Urai (1987, fig. 6). Subgrain boundaries of this type are called Type IV subgrain boundaries by Means & Ree (1988). *Amalgamation* occurs in Fig. 2(b & c) where the grain boundary between grains 4 and 5 degenerates, by progressive *reduction* of misorientation, into a subgrain boundary (Type III of Means & Ree 1988). This is the opposite of the lattice rotation process in 'rotation recrystallization' (Guillope & Poirier 1979), that creates a grain boundary from a subgrain boundary. In the

steady state, it is probably some balance between dissection and rotation of large subgrains (which locally reduce grain size) and coalescence, amalgamation and dynamic grain growth (which locally increase grain size) that maintains the constant average grain size.

Another newly-recognized process is *grain migration* (Urai *et al.* 1986, Urai 1987, fig. 8). Here a whole grain migrates through the material, such that it eventually encloses none of the atoms it originally contained (except perhaps for the odd diffusing atoms that have been swept along with it). The best example of grain migration in Fig. 2 is provided by the 7 part of the supergrain 7–38 in Fig. 2(c). This grain originally enclosed atoms that are now mostly in grain 6.

Grain-size increase during dynamic recrystallization at constant temperature was first recognized using synkinematic microscopy by Jessell (1986a). This presumably occurs when the initial grain size is less than the steady-state grain size for the stress level imposed. One wonders whether the grain size in some wallrocks hosting mylonites was gradually increasing (under the influence of low strain rate) at the same time as the grain size in the mylonites was decreasing (under the influence of relatively high strain rate)? In a case like this the wallrock in its present condition would not be the microstructural protolith of the mylonite, but a coarsened version of the real protolith.

A central problem in understanding dynamic recrystallization is understanding what controls the migration direction of each mobile grain boundary. A start has been made on this by Jessell (1986a). He used marker particles in OCP to calculate the accumulated strain either side of a mobile boundary and measured the basal plane orientation of each grain. From these two measured quantities he estimated an 'energy function' for each grain, representing the plastic strain energy stored in the grain. Thirty-seven grain-pairs were checked in this way to see whether the more energetic grain was consumed by the less energetic grain, as one would expect for the most rapid reduction of the local strain energy. The predicted direction of grain boundary migration matched the observed direction for 30 of the 37 grain-pairs. Means & Jessell (1986) have described the two-dimensional theory for grain boundary migration where it occurs solely to prevent strain incompatibility between grains, which tend to arise in materials of low crystallographic symmetry on account of limited slip systems and different lattice orientations. It is not known yet whether this 'accommodation migration' is ever important in dynamic recrystallization, but one grain boundary behaving this way was recognized in OCP using synkinematic microscopy.

A curious phenomenon recorded by Urai (1983a, 1987) and Tungatt & Humphreys (1984) is reversal in the direction of grain boundary migration. Grain A consumes B for a while and then B consumes A, along the same portion of their mutual boundary. An explanation has been suggested by Urai (1987), but much remains to be learned about the factors governing the rate and direction of dynamic grain boundary migration.

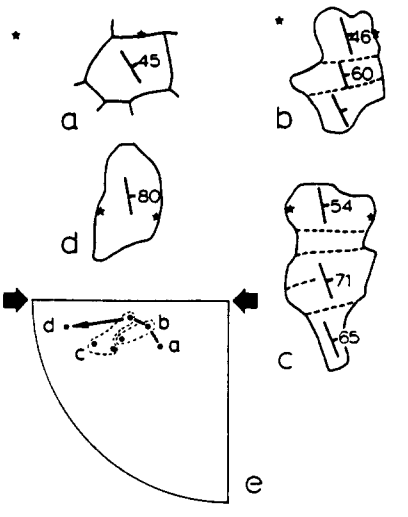

Fig. 3. Changing shape and basal plane orientation of grain 6 at stages (a–d) of Fig. 2. Stars mark positions of two silicon carbide particles and indicate local horizontal shortening at each stage. (e) SW quadrant of a lower hemisphere stereographic projection showing the *c*-axis trajectory (solid arrow) for the portion of grain 6 nearest the stars, and for other subgrains. The *c*-axis moves toward the shortening direction (stubby arrows).

Synkinematic microscopy has also begun to cast new light on the development of lattice preferred orientation in flowing polycrystals. Means (1983) and Jessell (1986a) have measured *c*-axis reorientation trajectories in OCP by interrupting deformation experiments and measuring crystallographic orientations with a universal stage. Figure 3 shows another example of this, for grain 6 in Fig. 2. Although the interruption of deformation is undesirable, information on trajectories and on the strain fields within and between grains (Jessell 1986a) is going to be useful for refining and checking models such as the Taylor model for lattice preferred orientation (see Lister *et al.* 1978, Jessell 1986 a, b). Even before-and-after U-stage measurements, without the connecting trajectories (as obtained for sheared ice by Burg *et al.* 1986), are valuable. Wilson (1986) has shown that comparable ice fabrics are obtained in experiments on bulk samples and in experiments on thin samples observed synkinematically. This encourages further use of synkinematic microscopy in fabric studies.

Two other research areas in which synkinematic microscopy has already made contributions are elucidation of details of crystal–plastic deformation processes, especially intracrystalline kinking, and exploration of the influence of a solvent fluid on deformation processes and strength. Geological work in the first area was started by McQueen *et al.* (1980), who deformed stibnite with *reflected light* synkinematic microscopy. It has been continued particularly by the ice workers (Burg *et al.* 1986, Wilson 1986, Wilson *et al.* 1986). Experiments with a solvent fluid have been carried out by Urai (1983, 1987), who found that the presence of even small amounts of water (as grain boundary films) in carnallite and bischofite dramatically reduces strength and enhances grain boundary mobility.

TEACHING APPLICATIONS

Synkinematic microscopy lends itself to teaching because simplified apparatus can be used, like the hand-operated press in Fig. 5(c), and some of the organic sample materials are readily accessible and easy to handle, particularly paradichlorobenzene. Means (1986) describes student exercises for which no press is required. The samples are deformed by twisting the windows directly with the fingers. Jessell & Means (1986) have employed another torsion apparatus, this one specifically for use with norbornene, a material that behaves at room temperature like OCP but moves its grain boundaries much faster (relative to the deformation rate). Norbornene is very volatile and foul-smelling, so the norbornene deformation cell is sealed.

Several videotapes made by synkinematic microscopy are available. Inquiries should be addressed to C. J. L. Wilson, Department of Geology, University of Melbourne, Parkville 3051, Australia; J. L. Urai, Institute of Earth Sciences, State University of Utrecht, Box 80.021, 3508TA Utrecht, The Netherlands; R. J. Knipe, Department of Earth Sciences, University of Leeds, Leeds LS2 9JT, U.K.; B. Van der Pluijm and A. Schedl, Department of Geological Sciences, University of Michigan, Ann Arbor, MI 48109, U.S.A.

FUTURE DEVELOPMENTS

Both technically and scientifically, synkinematic microscopy to date has only scratched the surface of what is possible. Some means of measuring stress in the sample can probably be devised. R. J. Knipe (personal communication 1982) has attempted this by fixing a strain gauge to one of the windows, in an apparatus using the loading principle of Fig. 1(d). Methods for measuring lattice orientations without interrupting the deformation can also be devised (for example by using flat stage extinction directions and birefringence measurements). The technique can certainly be adopted to operation in the creep mode (constant stress) in addition to the present constant strain rate mode. This is one way to control stress in the specimen, leaving the easy-to-measure strain rate as the dependent variable. The most difficult technical problems have been, and will continue to be, problems of sample preparation and sample selection. Sodium nitrate, for example, is a nice calcite analog, but it is not easy to prepare thin samples of this material with a good foam texture, and once prepared, the samples often stick to the windows, even with silicone oil films to lubricate the interfaces.

The remaining figures in this paper have been picked to illustrate some scientific directions for future experiments. There is still much scope for observation of processes active in ductile shear zones. Figure 5(a & b) shows two moments in the life of a narrow, dextral, mylonite zone in paradichlorobenzene, being sheared at $10^{-5}\,s^{-1}$ room temperature. Note the crisp resolution of microstructural details. The zone of high strain-rate extends horizontally across the center of the photographs, between the two stars. Above and below the stars, the sample is more or less a single-crystal material, with many, well-defined subgrains. The stars are fixed relative to silicon carbide marker particles (the black specks). Their change in relative positions shows the increment of shear strain (about 0.3) between the two pictures. The white pointers in (a) indicate two grains that have grown much bigger in (b). The pointer in (b) indicates a grain that originated by pinching off of a small-wavelength grain boundary bulge that can be seen in (a). There is still much to be learned about how new grains form, both by bulge processes and by the process involving progressive rotation of subgrains (Fig. 4i–l). Close examination of pictures like Fig. 5(a & b) often reveals unexpected phenomena—like consumption *by the host* crystal of its own progeny (the newly-formed fine grains recently grown from the host). There is an example of this in Fig. 5(a & b), near the lower star.

Synkinematic microscopy has not been applied much to the study of brittle behavior, or to transitional behaviors between microscopically brittle and microscopically ductile behaviors, but there is obviously a field of interest here. Figure 5(d–g) shows the birth of a rupture zone in polycrystalline sodium nitrate, sheared using the hand-operated press (Fig. 5c) at room temperature. Again, the stars are fixed to material points and show the accumulating dextral displacement. Frame 5 (d) shows the appearance of the damaged zone after a displacement of about 5 μm. There are dilated, intergranular cracks (white pointer) and *e* twin lamellae (black pointer). Subsequent pictures show widening of the damaged zone, without the appearance yet of any single, narrow surface across which the velocity jump occurs. A rupture zone has formed but no fault has propagated through it. Note the intergranular fractures (white pointer) in (g) extending outside the granulated (dark) zone. Figure 5(h–k) shows further details of incipient faulting in a coarser specimen. A rhombohedral cleavage crack (white pointer in h) dilates in (i) and (j), then closes again in (k). A crack visible in (h) at the black pointer closes tight or heals in subsequent photographs. Twinning intensification occurs in the large grain, upper right. Further work on rupture zone and fault development, with and without a solvent fluid present, is obviously worthwhile, especially if a way can be found to control the normal stress acting in the plane of the sample perpendicular to the deformation zone.

Another potentially fertile area is study of deforming polycrystals with a void population, with and without fluids in the voids (Ree 1988). Figure 6(a–f) shows voids in an OCP sample being sheared dextrally at 65°C, $10^{-5}s^{-1}$. The voids are the intergranular regions marked out by dark boundaries in the plain light photographs (a) and (b). A few voids were present in the starting material, but most were deformation-induced. They lean preferentially 'against' the direction of shear, as is to be expected. Although the total void area is about constant, the size and shape of individual voids can change markedly as deformation progresses. See, for

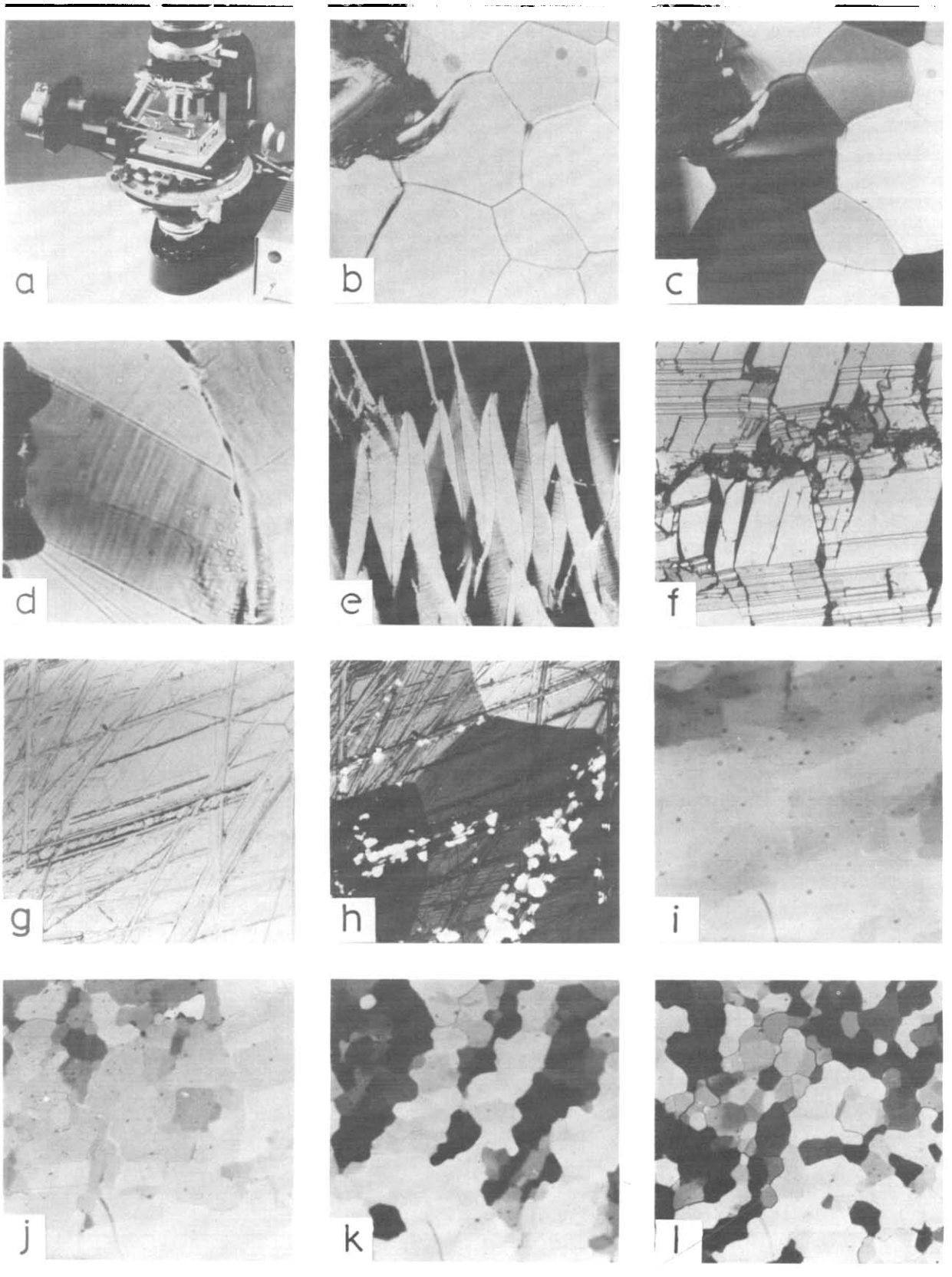

Fig. 4. (a) Urai press on microscope stage; corner of control box lower right. (b) Needle track, upper left, on uncovered OCP sample, plain light. (c) Crossed polars view of same field showing crystal–plastic microstructures. Photograph edge 1.3 mm. (d) Deformation band in OCP grain (dipping right) with features similar to deformation lamellae in quartz (dipping left). Photograph edge 0.5 mm. (e) Kink bands in biphenyl single crystal. Photograph edge 1.5 mm. (f) Rhombohedral cleavage cracks (steeply-dipping) with *e* twin lamellae (gently-dipping) in sodium nitrate. Photograph edge 1.5 mm. (g) OCP polycrystal scratched with tissue paper. Plain light. (h) Crossed polars view of (g) showing coarse original grains and fine, recrystallized grains along the scratches. Photograph edge 1.5 mm. (i–l) Rotation recrystallization of a sodium nitrate single crystal at 300°C, during horizontal, dextral shearing with γ about 1.5. (Unpublished experiment by J. Urai.)

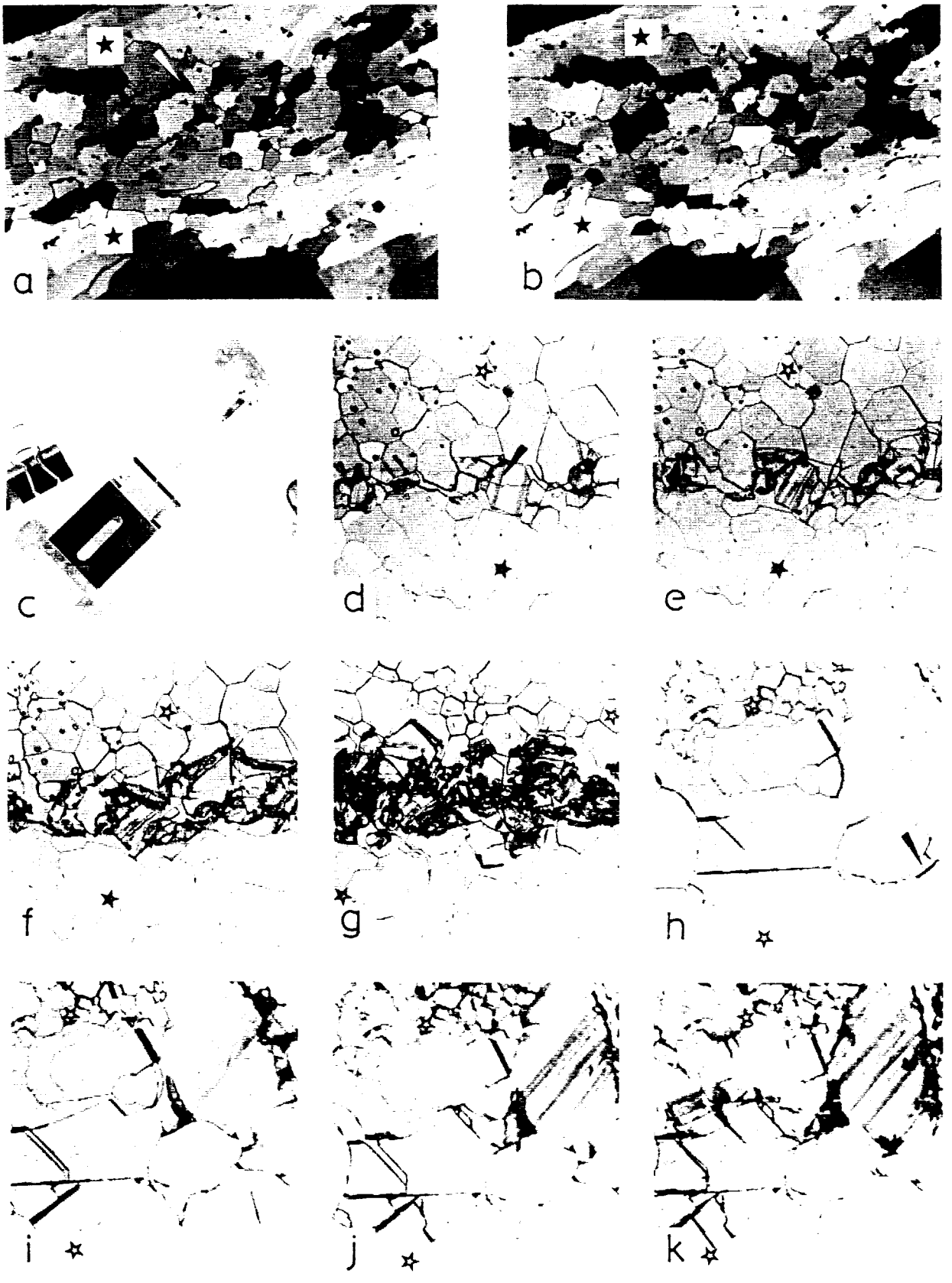

Fig. 5. (a & b) Horizontal, dextral shear zone (between stars) in paradichlorobenzene. Crossed polars. Photograph short edge 1.3 mm. A shear strain increment of about 0.3 accumulated between the two photographs. Shear strain (a) >1 but unknown. (c) Hand-operated press for use on student microscopes. Overall length is 16 cm. (d–g) Development of a rupture zone in dextrally sheared sodium nitrate. Stars fixed to material, show displacement. Photograph edge 0.5 mm. (h–k) Similar features in a coarser sodium nitrate sample. Photograph edge 0.5 mm.

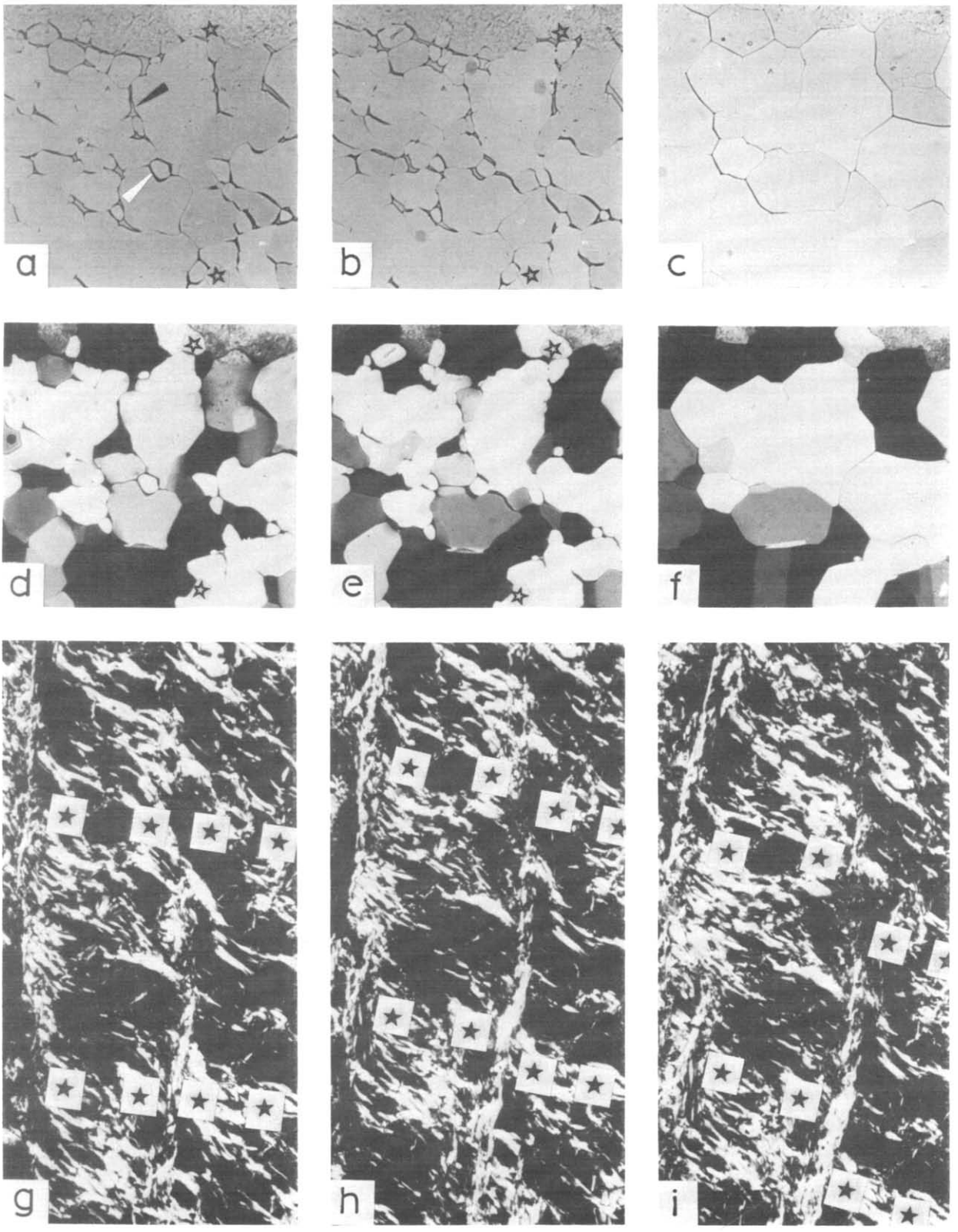

Fig. 6. (a & b) and (d & e) Plain light and crossed-polars views of a dextrally shearing OCP specimen with intergranular voids (pointers in a). Shear strain already accumulated in (a) about 1. Stars show displacements. (c) & (f) Same fields as (b) & (e) after a 16-hour static recovery period. Photograph edges 1.3 mm. (Unpublished experiment by J. H. Ree.) (g–i) Three views of active *S–C* fabric development in dextrally shearing paraffin wax. Shearing direction up to left down to right, on the page. Photograph short edge 0.5 mm.

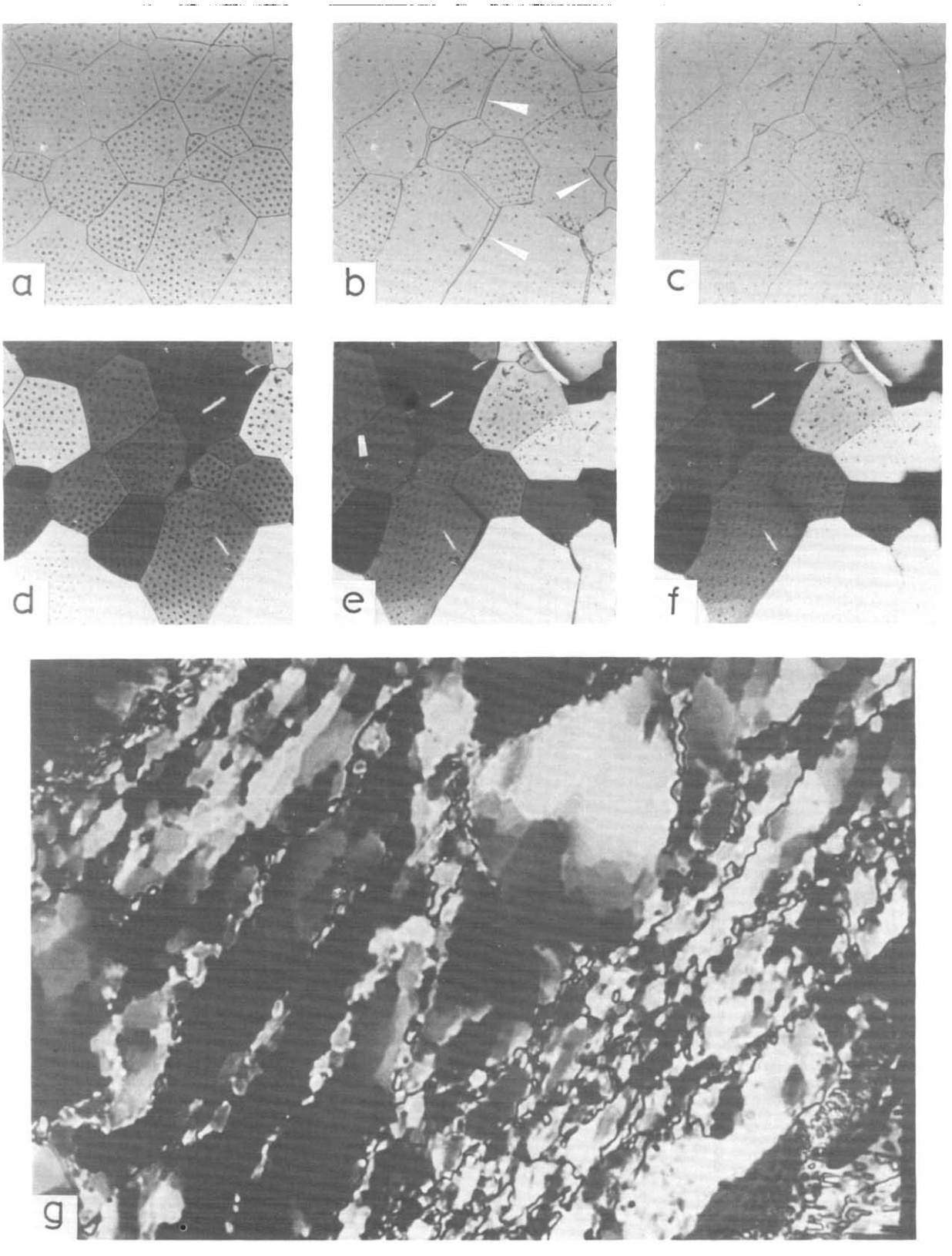

Fig. 7. (a–f) Cracking and melt-healing in OCP. Photograph edges 1.3 mm. (g) A room temperature, thymol 'tectonite'. Photograph short edge 1.3 mm.

example, closure of the void at the black pointer in (a) and dilation of the void at the white pointer. The patterns of void shape-change are consistent with grain boundary sliding as a deformation mechanism here, but it is not certain that this process has operated (in the absence of marker particles in this specimen). What *is* happening, simultaneously with the void evolution, is plastic deformation of at least some of the grains and grain boundary migration. Plastic deformation is indicated by development of uneven interference shades in the grains. Grain boundary migration occurs for example around the black dot on the left margin of (d), where a grey grain consumes part of the white grain just below it. The mix of deformation processes in 6(a & b) thus includes plastic deformation of the grains, dynamic recrystallization, void growth and shrinkage and probably grain boundary sliding. Figure 6(c & f) shows the same area as (b & e) 16 hours after the deformation was stopped at condition (b). During this time the sample was held at the deformation temperature of 65°C. The voids have vanished. If this was a rock, pity the geologist who seeks to work out what was happening in (a) and (b) from what he sees in (c). A virtue of synkinematic microscopy is that one *knows* the microstructure of the as-deformed material and can clearly distinguish between this and the microstructure as modified postkinematically. 'Stripping away' postkinematic effects is a necessary task for geologists, and one that will become easier the more experience we gain of postkinematic processes and their signatures using the present technique.

Another application for synkinematic microscopy is to the study of strain rate heterogeneity in deforming materials (see also Knipe 1989). Figure 6(g–i) shows three stages in the history of a piece of paraffin wax deforming heterogeneously and developing two foliations. The sample was being sheared vertically, down to the right-hand side in the photographs. A shear-parallel *C* foliation is developing (dipping steeply left) along with an oblique *S* foliation (dipping moderately right). Eight stars in (g) are positioned on marker particles visible in a plain light photo of the same field. They make two, more or less straight, lines normal to the *C* surfaces. One can see the progressive offset of these material lines across the right-hand *C* surface in (h) and (i). One can also see (from the changing distances between stars measured parallel to the *C* surfaces) that the material between the *C* surfaces is shortening vertically, simultaneously with shear along the *C* surfaces. This is an example of a complex, but I imagine common, kind of shear zone behavior, in which shear zones change length while they shear because the whole material in which they are embedded is deforming (see also Ramsay 1980, fig. 3, Means 1977, 1988).

Another application is to the study of deforming crystal–melt systems. Figure 7(a–f) shows a specimen of OCP at its melting point. There is an invisible melt film between the sample and the glass and numerous melted-out holes or depressions in the crystals (the regularly-shaped dark spots). Frame (a) shows the undeformed condition, (b) shows the same field after a small deformation and intergranular cracks (white pointers) that have dilated and (c) shows the same field a few minutes later, when melt-healing has occurred, re-establishing an undeformed-looking polygonal microstructure. Here is another microstructure with a short memory of previous microstructural states.

Probably the most exciting future developments will come as synkinematic microscopy moves from single-phase samples to samples consisting of several phases which react chemically with each other to produce porphyroblasts of new phases. A step toward the study of these *dynamically reactive* systems is to study dynamic phase change in a one-component system. For example, paradichlorobenzene inverts at 31°C from a monoclinic form stable at room temperature to a triclinic form stable up to the 52°C melting point. The two phases are readily distinguished optically, by the higher birefringence of the triclinic form. It will be interesting, for example, to begin deforming the monoclinic material at room temperature and then, while deformation continues, to gradually turn up the temperature until porphyroblasts of the triclinic phase begin to grow synkinematically. Experiments on two-phase, non-reactive OCP–camphor samples have been started by C. K. Mawer (personal communication 1986) and by ter Haar *et al.* (unpublished abstract, EUG IV Conference, 1987), and ice–mica, ice–camphor and ice–naphthalene results have already been published by Wilson (1984) and Burg & Wilson (1987).

I conclude by directing attention to Fig. 7(g). This could be a marble, or a dunite, or a quartzite, or a plagioclase rock from a natural high-strain zone. But it is in fact a thymol ($CH_3(C_3H_7)C_6H_3OH$) polycrystal viewed synkinematically at room temperature. The appeal of this microstructure is not just in the geological-looking porphyroclasts and their subgrains and the strings of 'mortar', but the fact that one can make something like this in an afternoon, with inexpensive equipment, and *observe* whether or not there is shear parallel to the mortar strings, and what the sense of shear is, and whether the 'porphyroclasts' really are being progressively turned into mortar, and so on. One can check on current ideas about the significance of microstructure, and maybe improve on them. I once deformed a thymol specimen which first yielded brittly, to produce a cataclasite and then transformed itself, by plastic deformation of the fragments, dynamic recrystallization, and void-healing into a mylonitic material, not very different from Fig. 7(g). This recalls the brittle-to-plastic history for shear zones in granite as interpreted by Segall & Simpson (1986), and reminds us again that some microstructures in rocks may have short memories of complex histories.

Acknowledgements—I thank Mark Jessell, Rob Knipe, Chris Mawer, Jin Han Ree, Sue Treagus, Janos Urai and Chris Wilson for help with the text, and Ree and Urai for permission to use Figs. 6(a–f) and 4(i–l), respectively. Supported by U.S. National Science Foundation Grant EAR 85 06810.

REFERENCES

Burg, J. P. & Wilson, C. J. L. 1987. Deformation of two phase systems with contrasting lithologies. *Tectonophysics* **135**, 199–205.

Burg, J. P., Wilson, C. J. L. & Mitchell, J. C. 1986. Dynamic recrystallization and fabric development during simple shear deformation of ice. *J. Struct. Geol.* **8**, 857–70.

*Dong, H. 1985. A possible formational process of mylonite. *Acta Geologica Sinica* **4**, 286–293 (in Chinese).

Guillope, M & Poirier, J. P. 1979. Dynamic recrystallization during the creep of single-crystalline halite: an experimental study. *J. geophys. Res.* **84**, 5557–5567.

Haessner, F. & Hoffman, S. 1978. Migration of high angle grain boundaries. In: *Recrystallization of Metallic Materials* (edited by Haessner, F.). Dr. Rieder Verlag, Stuttgart, 63–95.

Jessell, M. W. 1986a. Grain boundary migration and fabric development in experimentally deformed octachloropropane. *J. Struct. Geol.* **8**, 527–542.

*Jessell, M. W. 1986b. Dynamic grain boundary migration and fabric development: observations, experiments, and simulations. Unpublished Ph.D. thesis, State University of New York at Albany.

Jessell, M. W. & Means, W. D. 1986. Deformation and recrystallization microstructures in quartz: a new teaching simulation. *Geol. Soc. Am. Abs. w. Prog.* **18**, 646.

Knipe, R. J. 1989. Deformation mechanisms–recognition from natural tectonites. *J. Struct. Geol.* **11**, 127–146.

Lister, G. S., Paterson, M. S. & Hobbs, B. E. 1978. The simulation of fabric development in plastic deformation and its application to quartzite: the model. *Tectonophysics* **45**, 107–145.

McQueen, D. R., Kelly, W. C. & Clark, B. R. 1980. Kinematics of experimentally produced deformation bands in stibnite. *Tectonophysics* **66**, 55–81.

Means, W. D. 1977. A deformation experiment in transmitted light. *Earth Planet Sci. Lett.* **35**, 169–179.

*Means, W. D. 1980. High temperature simple-shearing fabrics: a new experimental approach. *J. Struct. Geol.* **2**, 197–202.

Means, W. D. 1981. The concept of steady-state foliation. *Tectonophysics* **78**, 179–199.

Means, W. D. 1983. Microstructure and micromotion in recrystallization flow of octachloropropane: a first look. *Geol. Rdsch.* **72**, 511–528.

Means, W. D. 1986. Three microstructural exercises for students. *J. geol. Education* **34**, 224–230.

Means, W. D. 1988. Stretching faults in paraffin wax. *Geol. Soc. Am. Abs. w. Prog.* **20**, A215.

*Means, W. D. & Dong, H. 1982. Some unexpected effects of recrystallization on the microstructures of materials deformed at high temperature. *Mitt. geol. inst. ETH*, Neue Folge **239a**, 205–207. (Also in *Kexue Tongbao* **31**, 402–404, 1986.)

Means, W. D. & Jessell, M. W. 1986. Accommodation migration of grain boundaries. *Tectonophysics* **127**, 67–86.

Means, W. D. & Ree, J. H. 1988. Seven types of subgrain boundaries in octachloropropane. *J. Struct. Geol.* **10**, 765–770.

Means, W. D. & Xia, Z. G. 1981. Deformation of crystalline materials in thin section. *Geology* **9**, 538–543.

*Mosher, S., Berger, R. L. & Anderson, D. E. 1975. Fracturing characteristics of two granites. *Rock Mech.* **7**, 167–176.

Mugge, O. 1898. Ueber translationen und verwandte erscheinungen in kristallen. *Neues Jb. Miner. Geol. Palaeont.* **1**, 71–158.

*Opstal, K. van 1984. In situ observatie van simple shear experimenten met σ- en β-para-dichlorobenzeen. Unpublished M.Sc. thesis, University of Amsterdam.

Ramsay, J. G. 1980. Shear zone geometry: a review. *J. Struct. Geol.* **2**, 83–99.

Ree, J. H. 1988. Evolution of deformation-induced grain boundary voids in octachloropropane. *Geol. Soc. Am. Abs. w. Prog.* **20**, A213.

Rigsby, G. P. 1960. Crystal orientation in glaciers and experimentally deformed ice. *J. Glaciol.* **3**, 589–606.

*Schedl, A. & Van der Pluijm, B. A. 1987. Deformation of rock analogues—video instruction in deformation microstructures. *Geol. Soc. Am. Abs. w. Prog.* **20**, 740.

Segall, P. & Simpson, C. 1986. Nucleation of ductile shear zones on dilatant fractures. *Geology* **14**, 56–59.

Sherwood, J. N. 1979. Lattice defects, self-diffusion, and the plasticity of plastic crystals. In: *The Plastically Crystalline State* (edited by Sherwood, J. N.). Wiley-Interscience, New York, 39–83.

Steinemann, S. Von 1958. Experimentelle untersuchung zur plastizitat von eis. *Beit. zur Geol. der Schweiz, Hydrologie* **10**, 4–72.

Tungatt, P. D. & Humphreys, F. J. 1981a. An *in situ* optical investigation of the deformation behavior of sodium nitrate— an analogue of calcite. *Tectonophysics* **78**, 661–676.

*Tungatt, P. D. & Humphreys, F. J. 1981b. Transparent analogue materials as an aid to understanding high temperature polycrystalline plasticity. In: *Deformation of Polycrystals: Mechanisms and Microstructures* (edited by Horsewell, A., Leffers, T. & Lilholt, H.). Riso Nat. Lab., Roskilde, 393–398.

Tungatt, P. D. & Humphreys, F. J. 1984. The plastic deformation and dynamic recrystallization of polycrystalline sodium nitrate. *Acta metall.* **32**, 1625–1635.

Urai, J. L. 1983a. Water-assisted dynamic recrystallization and weakening in polycrystalline bischofite. *Tectonophysics* **96**, 125–157.

*Urai, J. L. 1983b. Deformation of wet salt rocks. Unpublished Ph.D. thesis, State University of Utrecht, The Netherlands.

Urai, J. L. 1987. Development of microstructure during deformation of carnallite and bischofite in transmitted light. *Tectonophysics* **135**, 251–263.

*Urai, J. L. & Humphreys, F. J. 1981. The development of shear zones in polycrystalline camphor. *Tectonophysics* **78**, 677–685.

Urai, J. L., Humphreys, F. J. & Burrows, S. E. 1980. *In situ* studies of the deformation and dynamic recrystallization of rhombohedral camphor. *J. Mater. Sci.* **15**, 1231–1240.

Urai, J. L., Means, W. D. & Lister, G. S. 1986. Dynamic recrystallization of minerals. In: *Mineral and Rock Deformation: Laboratory Studies—The Paterson Volume* (edited by Heard, H. C. & Hobbs, B. E.). *Am. Geophys. Un. Geophys. Monogr.* **36**, 161–199.

Wakahama, G. 1964. On the plastic deformation of ice V, Plastic deformation of polycrystalline ice. *Low Temperature Sci.* **22**, 1–24.

Wilson, C. J. L. 1984. Shear bands crenulations, and differentiated layering in ice-mica models. *J. Struct. Geol.* **6**, 303–319.

Wilson, C. J. L. 1986. Deformation-induced recrystallization of ice: the application of *in situ* experiments. In: *Mineral and Rock Deformation: Laboratory Studies—The Paterson Volume* (edited by Heard, H. C. & Hobbs, B. E.). *Am. Geophys. Un. Geophys. Monogr.* **36**, 213–232.

Wilson, C. J. L., Burg, J. P. & Mitchell, J. C. 1986. The origin of kinks in polycrystalline ice. *Tectonophysics* **127**, 27–48.

---

*Entries not referred to in text, included for completeness as bibliography of work to date.